

Optically Pumped Lasing in Solution-Processed Perovskite Semiconducting Materials: Self Assembled Fabry-Pérot Microcavity

Fumio Sasaki¹, Ying Zhou¹, Yoriko Sonoda¹, Reiko Azumi¹, Hiroyuki Mochizuki², Van-Cao Nguyen³, and Hisao Yanagi³

¹Electronics and Photonics Research Institute, National Institute of Advanced Industrial Science and Technology (AIST).

1-1-1 Umezono, Tsukuba, Ibaraki 305-8568, Japan

Phone: +81-29-861-5475 E-mail: f-sasaki@aist.go.jp

²Research Center for Photovoltaics, AIST, 1-1-1, Higashi, Tsukuba, Ibaraki 305-8565, Japan

³Graduate School of Materials Science, Nara Institute of Science and Technology (NAIST), 8916-5 Takayama, Ikoma, Nara 630-0192, Japan

Abstract

Optical pumped lasing has been observed in solution-processed perovskite semiconducting materials, $\text{CH}_3\text{NH}_3\text{PbBr}_3$. Self-assembled Fabry-Pérot (FP) cavities have been easily obtained by using a simple ‘cast-capping method’. The observed spectra show clear multi-mode lasing of FP cavities under pulsed optical pumping. The mode intervals are well explained by the optical constants with large dispersions of the materials.

1. Introduction

Solution processed fabrication methods of semiconducting materials are very important for the low cost and large area devices [1]. Recently, metal halide perovskite type organic photovoltaic devices have greatly progressed and power conversion efficiency showed nearly 20% conversion efficiency, indicating the most promising materials for solution-processed photovoltaic cells [2-4]. Perovskite materials with lead halide systems also exhibit laser emissions under the optical pumping [5-8] and LED devices [9, 10]. These facts enable us foreseeing the realization of current-injected lasing devices in solution-processed fabrication.

Perovskite microcrystals fabricated by using the vapor phase methods showed clear whispering gallery mode (WGM) lasing under the optical pumping, because they have quite clear optical cavity [11]. Nanowire microcavities precipitated from the solutions of methylammonium (MA) species showed high Q value and very low threshold of lasing [12]. We also reported microdisk lasing under the optical pumping in the microcrystals fabricated by casting [13]. Here, we report the growth of large size crystalline Fabry-Pérot (FP) cavities and their optically pumped lasing of MAPbBr_3 material. The lasing spectra show clear multi-mode oscillation and we can determine the effective index around the lasing spectral area.

2. Sample Preparations

In the sample preparation, we used so called cast-capping method, described below. Methylammonium bromide ($\text{CH}_3\text{NH}_3\text{Br}$, Wako, 99.999%) and PbBr_2 (Sigma-Aldrich, 99.999%) powders were solved into *N,N*-dimethylformamide (DMF) without further purifica-

tion. The equimolar amount of $\text{CH}_3\text{NH}_3\text{Br}$ and PbBr_2 from 50 to 500 mM was used. The powders were completely dissolved in DMF at RT after washing with diethyl ether. The solutions were casted on indium tin oxide (ITO) layers sputtered on Si/SiO₂ substrates or bare SiO₂ substrates. After the casting, we put another substrate on it, as shown in Fig. 1. It took a few hours until the film was completely dried at RT in the cast case, while it took 1-10 days until the film was completely dried at RT to 80 °C in the cast-capping case. All of the fabrication processes were carried out in ambient air.

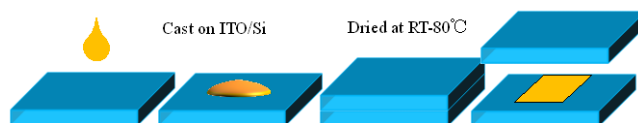


Fig. 1 Schematic drawing of fabrication processes of the cast-capping method.

3. Optical Experiments

We have carried out the optical experiments under the pulsed excitation on the MAPbBr_3 FP cavities at 397 nm with a pulse width of 200-300 fs and a repetition rate of 1 kHz. All the optical experiments have been carried out at RT in ambient air. The left part of Fig. 2 shows fluorescent microscope images of FP cavities with the cavity length of 20 (upper) and 49 (lower) μm , respectively. The bright spots were observed at both sides of FP cavities, indicating lasing, as shown in the images. The right part of Fig. 2 shows the lasing spectra of both cavities. The mode numbers increase with the increase of the cavity size. However, the mode interval is not regular in the observed spectra. In a FP cavity, the horizontal length is the cavity length, L and the lasing mode interval ΔE is expressed as [14]

$$\Delta E = E_{m+1} - E_m = \frac{hc}{2n_{\text{eff}}L}, \quad n_{\text{eff}} = \left(n + E \frac{dn}{dE} \Big|_{E_m} \right) \quad (1)$$

where $E_m = mhc/nL$ is the energy of the m -th mode, h is the Planck constant, c is the velocity of light in vacuum, n_{eff} is the effective refraction index, and n is the refraction index of the gain materials, respectively. We estimated the

effective index from Eq. (1), as shown in Fig. 3. Results are slightly scattered, but a slight slope is seen in the figure. The slope of n_{eff} , namely, n_{eff} decreases with the decrease of the photon energy, comes from the dispersion of the materials.

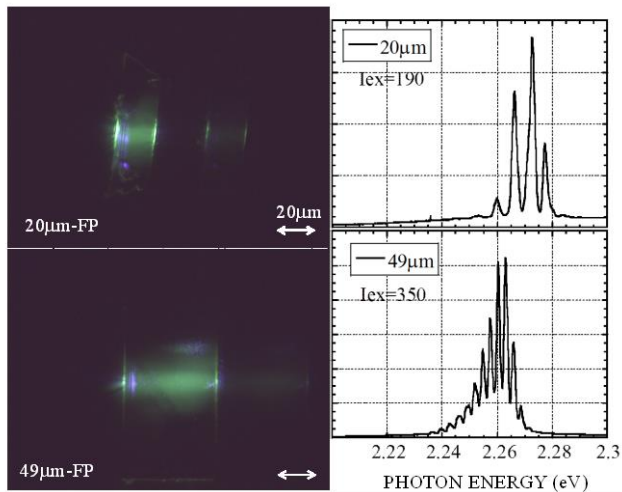


Fig. 2 Fluorescence images of the FP cavities (left part). The right part shows lasing spectra of the $\text{CH}_3\text{NH}_3\text{PbBr}_3$ self-assembled FP cavities. The excitation density, I_{ex} is shown in each figure in the unit of μJcm^{-2} .

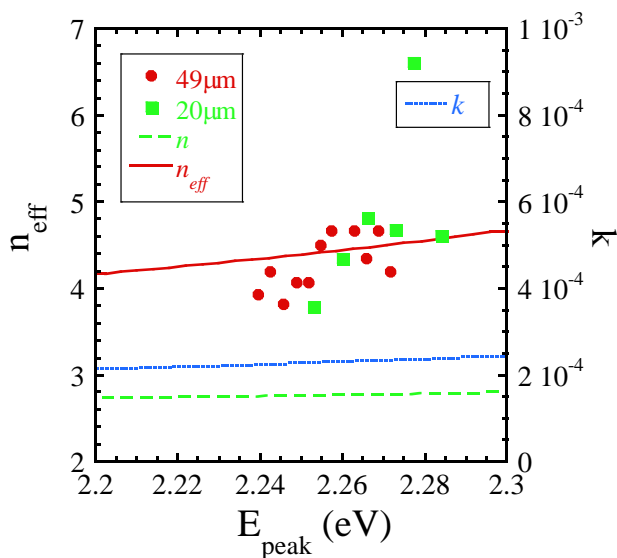


Fig. 3 Effective index observed in the FP cavities and fitted value indicated by the solid line.

The optical constant of perovskite materials has been reported and the refractive index around the band gap of $\text{CH}_3\text{NH}_3\text{PbI}_3$ is approximately 2.4 [5]. The strong absorption band exists just above the gap, so that n_{eff} is influenced by the absorption dispersion, as we previously reported [13]. In the present case, the observed n_{eff} of 4 – 5 in the FP cavities can also be explained the strong absorption band of

$\text{CH}_3\text{NH}_3\text{PbBr}_3$ [15]. Details will be presented in the conference.

Acknowledgments

This work was partly supported by JSPS KAKENHI Grant Number 25390060.

References

- [1] J. A. Rogers, T. Someya, Y. Huang, *Science* **327**, 1603 (2010).
- [2] M. M. Lee, J. Teuscher, T. Miyasaka, T. N. Murakami, H. J. Snaith, *Science* **338**, 643 (2012).
- [3] H. Zhou, Q. Chen, G. Li, S. Luo, Tze-bing Song, H.-S. Duan, Z. Hong, J. You, Y. Liu, and Y. Yang, *Science* **345**, 542 (2014).
- [4] W. S. Yang, J. H. Noh, N. J. Jeon, Y. C. Kim, S. Ryu, J. Seo, and S. I. Seok, *Science* **348**, 1234 (2015).
- [5] G. Xing, N. Mathews, S. S. Lim, N. Yantara, X. Liu, D. Sabba, M. Grätzel, S. Mhaisalkar and T. C. Sum, *Nat. Mater.* **13**, 476 (2014).
- [6] F. Deschler, M. Price, S. Pathak, L. E. Klintberg, D.-D Jarausch, R. Higler, S. Hüttner, T. Leijtens, S. D. Stranks, H. J. Snaith, M. Atatüre, R. T. Phillips, and R. H. Friend, *J. Phys. Chem. Lett.* **5**, 1421 (2014).
- [7] T. S. Kao, Yu-Hsun Chou, C.-H. Chou, F.-C. Chen, and T.-C. Lu, *Appl. Phys. Lett.* **105**, 231108 (2014).
- [8] D. Priante, I. Dursun, M. S. Alias, D. Shi, V. A. Melnikov, T. K. Ng, O. F. Mohammed, O. M. Bakr, and B. S. Ooi, *Appl. Phys. Lett.* **106**, 081902 (2015).
- [9] Z.-K. Tan, R.S. Moghaddam, M.L. Lai, P. Docampo, R. Higler, F. Deschler, M. Price, A. Sadhanala, L.M. Pazos, D. Credgington, F. Hanusch, T. Bein, H.J. Snaith, and R.H. Friend, *Nat. Nanotechnol.* **9**, 687 (2014).
- [10] Y.-H. Kim, H. Cho, J.H. Heo, T.-S. Kim, N. Myoung, C.-L. Lee, S.H. Im, and T.-W. Lee, *Adv. Mater.* **27**, 1248 (2014).
- [11] Q. Zhang, S.T. Ha, X. Liu, T.C. Sum, and Q. Xiong, *Nano Lett.* **14**, 5995 (2014).
- [12] H. Zhu, Y. Fu, F. Meng, X. Wu, Z. Gong, Q. Ding, M. V. Gustafsson, M. T. Trinh, S. Jin, and X.-Y. Zhu, *Nat. Mater.* **14**, 636 (2015).
- [13] F. Sasaki, H. Mochizuki, Y. Zhou, Y. Sonoda, and R. Azumi, *Jpn. J. Appl. Phys.* **55**, 04ES02 (2016).
- [14] K. Bando, S. Kumeta, F. Sasaki, and S. Hotta, *Jpn. J. Appl. Phys.* **50** (2011) 101603.
- [15] H. Kunugita, T. Hashimoto, Y. Kiyota, Y. Udagawa, Y. Takeoka, Y. Nakamura, J. Sano, T. Matsusita, T. Kondo, T. Miyasaka, and K. Ema, *Chem. Lett.* **44**, 852 (2015).